

STATE-OF-THE-ART ARTICLE

FIRST HUMAN IMAGING STUDIES WITH THE EXPLORER TOTAL-BODY PET SCANNER

^{1,2}Ramsey D. Badawi, ³Hongcheng Shi, ³Pengcheng Hu, ³Shuguang Chen, ⁴Tianyi Xu, ⁵Patricia M. Price, ⁴Yu Ding, ¹Benjamin A. Spencer, ¹Lorenzo Nardo, ⁴Weiping Liu, ⁴Jun Bao, ¹Terry Jones, ⁴Hongdi Li, ^{2,1}Simon R. Cherry

¹Department of Radiology, University of California Davis Medical Center, Sacramento, CA, USA

²Department of Biomedical Engineering, University of California, Davis, CA, USA

³Department of Nuclear Medicine, Zhongshan Hospital, Shanghai, China

⁴United Imaging Healthcare, Shanghai, China

⁵Department of Surgery and Cancer, Imperial College, London, U.K.

Corresponding Authors: Ramsey D. Badawi, Ph.D.
Department of Radiology
UC Davis School of Medicine
4860 Y Street
Sacramento,
CA 95817
USA

Phone: +1 916 703 2278
Email: rdbadawi@ucdavis.edu

Hongcheng Shi, M.D.
Department of Nuclear Medicine,
Zhongshan Hospital Fudan University,
180 Fenglin Rd,
Xuhui District
Shanghai,
China

Phone: +86 21 6404 1990
Email: shi.hongcheng@zs-hospital.sh.cn

Word Count: 3176

Figures: 7

Tables: 1

Financial Support: The EXPLORER scanner was developed with support from NCI, NIBIB and the NIH Office of the Director through Transformative R01 CA 206187, with additional support from United Imaging Healthcare. Support for the human imaging studies presented here was provided by United Imaging Healthcare and Zhongshan Hospital, Shanghai.

Running Title: *First Human Total-Body PET Studies*

ABSTRACT

Within the EXPLORER consortium, the construction of the world's first total-body PET/CT scanner has recently been completed. The 194 cm axial field of view of the EXPLORER PET/CT scanner is sufficient to cover, for the first time, the entire human adult body in a single acquisition in more than 99% of the population and allows total-body pharmacokinetic studies with frame durations as short as 1 second. The large increase in sensitivity arising from total-body coverage as well as increased solid angle for detection at any point within the body allows whole-body ^{18}F -fluorodeoxyglucose (^{18}F -FDG) PET studies to be acquired with unprecedented count density, improving the signal-to-noise ratio of the resulting images. Alternatively, the sensitivity gain can be used to acquire state-of-the-art diagnostic PET images with very small amounts of activity in the field of view (< 1 mCi), with very short acquisition times (~ 1 minute or less) or at later time points after the tracer's administration. We report here on the first human imaging studies on the EXPLORER scanner using a range of different protocols that provide initial evidence in support of these claims. These case studies provide the foundation for future carefully controlled trials to quantitatively evaluate the improvements possible through total-body PET imaging.

NOTEWORTHY

- First human studies on the EXPLORER total-body PET scanner.
- First medical imaging scanner of any kind capable of capturing 3D images of the entire human body at the same time.
- First study to show the kinetics of an injected radiotracer throughout the entire body.
- Diagnostic quality scans using acquisition times of ~ 1 minute or less.
- Diagnostic quality scans using injected doses less than 1 mCi
- Ability to image FDG distribution for up to 10 hours (< 5 half-lives) post injection.

INTRODUCTION

Current generation clinical PET/CT and PET/MR scanners typically cover an axial extent of 15-30 cm. Large increases in signal collection efficiency can be realized through extending the axial extent of the scanner, with the highest collection efficiency being approached as the scanner becomes long enough to cover the entire human body. A further key motivating factor for increasing the axial extent so dramatically is that it becomes possible to perform total-body dynamic studies, where tracer kinetic modeling with an image-derived input function to estimate model microparameters can be performed across all the organs and tissues of the body with high temporal resolution. Thus, the idea of developing long axial field of view scanners, and ultimately total-body scanners, has been studied over many years and has recently gained increasing traction, as reviewed in [1, 2].

In 2005, our team at UC Davis committed to developing a PET scanner long enough to simultaneously image the entire human body. Monte Carlo simulations suggested that the total-body imaging geometry could provide gains of up to 40-fold in effective count rate for total body applications compared to a more conventional 22-cm axial field of view scanner, if time-of-flight (TOF) effects are included [3, 4]. Gains of a factor of approximately 4-fold were predicted for single organ imaging. These gains could be used either to (a) deliver enhanced image quality, (b) reduce scan time, (c) increase the time-window after injection when scanning is possible, (d) reduce dose, or some combination of these.

In 2011, initial funding was obtained through the NCI's provocative questions award which facilitated the formation of the EXPLORER Consortium. This Consortium included teams from the University of Pennsylvania and Lawrence Berkeley National Laboratory as well as representatives from industry and a number of prominent imaging physician-scientists to guide planning. Subsequently, in 2015 we were awarded an NIH Transformative R01 grant which enabled us to partner with industry and begin construction. The EXPLORER Consortium is now

working on two devices, one with excellent timing resolution and a final projected length of 140 cm being developed by the University of Pennsylvania team in collaboration with KAGE Medical and Philips [5, 6], and the other with excellent spatial resolution and a length of 194 cm being developed by the UC Davis team and United Imaging Healthcare [7]. This second device is now complete, and is the first medical scanner of any kind that can acquire simultaneous static and dynamic three-dimensional images of the entire human body. Here we report the first total-body images acquired with human subjects on this scanner, which are intended to provide initial feasibility for each of the opportunities we had previously proposed, namely, improved image quality, fast scanning, delayed scanning after many half-lives, low-dose scanning and total-body pharmacokinetic imaging.

EXPLORER SCANNER:

The EXPLORER total-body PET/CT scanner (Figure 1) has an axial field of view of 194 cm and a transaxial field of view of 68.6 cm. It is integrated with an 80-row, 160 slice CT scanner. The PET detector crystals are made from lutetium (yttrium) oxyorthosilicate (LYSO) and measure $2.76 \times 2.76 \text{ mm}^2$ in cross-section by 18.1 mm in depth. Crystals are arranged in 7 x 6 arrays with a crystal pitch of 2.85 mm. Each array is read out using four $6 \times 6 \text{ mm}^2$ silicon photomultipliers. Additional information on the design and performance of the detector and electronics components may be found in [8]. The system is constructed as 8 axial units, each with an axial field of view of 24 cm, and with a gap of just 2.5 mm between units. The diameter of the detector ring is 78.6 cm, with a patient bore of 76 cm for the PET portion of the scanner. The system has time-of-flight (TOF) capability (timing resolution ~ 430 psecs), an energy resolution of 11.7%, and the reconstructed spatial resolution at 1 cm from the center of the field of view, using the NEMA NU-2 2018 protocol [9] and filtered back-projection reconstruction, is ~ 2.9 mm. A full physical and technical evaluation of the scanner will be forthcoming. All images

shown below are collected using a 430-645 keV energy window, accepting coincidences from detector pairs with unit differences up to ± 4 (corresponding to an axial acceptance angle of $\sim \pm 57^\circ$). The coincidence time window varies with unit difference to account for the different path lengths through the body and ranges from 4.5-6.9 ns. Reconstruction was carried out using a list-mode ordered subsets expectation maximization algorithm incorporating TOF and point spread function modeling (OSEM-TOF-PSF).

HUMAN SUBJECTS

Normal volunteer studies were performed in collaboration with Zhongshan Hospital, Shanghai. The study protocol was approved by the Zhongshan Hospital Ethics Committee and informed consent was obtained from all subjects. Exclusion criteria included: age < 18 years; exercise in the prior 24 hours; history of cancer, diabetes or bladder problems; inability to lie supine and still inside the scanner for the scan duration; inability to give informed consent; any employee of United Imaging Healthcare. All subjects were fasted for at least 6 hours prior to ^{18}F -FDG injection and scanning. Injections were either into an arm vein, or into a vein near the ankle. Demographics and injected activity are shown in Table 1. To explore the dynamic range of the scanner, subjects were injected with a range of doses of FDG and scans were acquired at a range of time intervals after injection. Subjects 1 and 2 were injected with standard activities based on weight (4.5 MBq/kg), while for subjects 3 and 4 the injected activity was reduced to $\sim 30\%$ and $\sim 10\%$ of the standard activity, respectively. Motion was minimized and repositioning was facilitated (where necessary) by use of evacuable positioning bags (model no. R7513-68NL, Klarity Medical Products, Inc., Newark, OH).

Low-dose CT scans were acquired for attenuation correction, and all corrections applied to the reconstructed images (randoms correction using delayed coincidence window, scatter correction, deadtime correction and detector normalization). All data were reconstructed using list-mode OSEM-PSF-TOF, with specific parameters given below.

HIGH-QUALITY IMAGING

Subject 1 was injected with 290 MBq of ^{18}F -FDG. At 82 minutes post-injection, a 20-minute list mode scan was initiated on the EXPLORER scanner. Data were reconstructed with 20 subsets and five iterations on a $1.0 \times 1.0 \times 1.45 \text{ mm}^3$ voxel grid.

Figure 2 shows a maximum intensity projection (MIP) and a sagittal slice through the image volume generated from the 20-minute scan. Of particular note is the uniformity of the uptake in the liver in the MIP image. Also shown are selected slices focusing on a range of anatomical features. It can be seen that the high count-density afforded by this scanner allows visualization of a range of small features without the drawback of high image noise.

REDUCED SCAN TIME

Total-body data from subject 1 was organized into list-mode datasets of duration 20 min, 10 min, 5 min, 2.5 min, 75 sec, 37.5 sec and 18.75 sec. The datasets were reconstructed with OSEM-PSF-TOF with 20 subsets and 2 iterations, on a voxel grid of $4.0 \times 4.0 \times 2.85 \text{ mm}^3$.

Representative slices from selected parts of the reconstructed volumes of these sequentially reduced datasets are shown in Figure 3. Unsurprisingly, the apparent noise increases as scan time is decreased, but the images appear to be of diagnostic quality at 37.5 seconds and are arguably diagnostic even at 18.75 seconds.

DELAYED IMAGING

Subject 2 underwent total-body PET scanning at 1 hr, 3 hrs, 8 hrs and 10 hrs post-injection. At each of the four time points, the scan duration was 14 minutes. The subject ate a planned low-carbohydrate meal after the 3-hour scan. The datasets were reconstructed with OSEM-PSF-TOF with 20 subsets and 2 iterations, on a voxel grid of $4.0 \times 4.0 \times 2.85 \text{ mm}^3$. Figure 4 shows MIPs and sagittal views from the repeated scans. Areas of focal intensity in the lower limb are from contamination. It can be seen that there is significantly more blood clearance at the 3-hour time-point compared to the 1-hour time-point. At ten hours post-injection, the injected activity

had decayed to 5.7 MBq; due to urinary excretion, less than this remained in the field of view. Even at this low amount of activity, the images appear to be of diagnostic quality. Of note, if 8.3 MBq were injected then, ignoring excretion, there would be 5.7 MBq in the field of view after one hour of uptake (similar to the amount in the subject at the 10-hour time-point); this would correspond to an effective dose of approximately 0.16 mSv [10].

LOW-DOSE IMAGING

Subject 4 was injected with 25 MBq of activity and scanned for ten minutes at 50 minutes post-injection. The datasets were reconstructed with OSEM-PSF-TOF with 20 subsets and 2 iterations, on a voxel grid of 3.125 x 3.125 x 2.85 mm³. Figure 5 shows a MIP and a coronal view. The images again appear to be of good quality. It should be noted that this subject was particularly small (43.5 kg; 152 cm).

SINGLE ORGAN IMAGING

Subject 3 was injected with 80 MBq of activity and scanned for 25 minutes starting at 25 minutes post-injection. The top of the subject's head was positioned approximately 30 cm away from the distal end of the axial field of view of the scanner. Brain images were reconstructed with OSEM-PSF-TOF with 20 subsets and 10 iterations, on a voxel grid of 1.2 x 1.2 x 1.45 mm³.

Figure 6 shows orthogonal slices through the brain image volume for subject 3. There is excellent delineation of the smaller structures of the brain, with the high sensitivity of the scanner supporting a very high resolution reconstruction without incurring a high noise penalty, even at this low injected dose.

TOTAL-BODY DYNAMIC IMAGING

Prior to the repeated scans performed on subject 2, data were acquired in list-mode as the subject was injected and subsequently for the next hour. Initial data were binned into frames of

one second in duration and reconstructed. Figure 7 shows selected frames from this scan, presented from frames within the rotating MIPs. The transit of the bolus from the heart, to the lungs, back to the heart and into the arterial tree can clearly be seen. Figure 7 also shows time-activity curves (TACs) generated from these images. Of particular note, the high temporal resolution of the scan series allows measurement of the dispersion between the left ventricle and the descending aorta (inset).

CONCLUSIONS

The potential benefits of and future applications for total-body PET rest on five primary claims, namely that a total body PET scanner can image better, faster, later after injection, and/or with lower dose; and that such a device can generate total-body dynamic images with high temporal resolution [1, 2]. Our initial data provide qualitative support for all these claims. Future studies will aim to provide quantitative assessments of these claims, to develop evidence for clinical utility, and to use this new and ground-breaking tool to answer questions in medicine and biology that hitherto could not be answered.

DISCLOSURE

United Imaging Healthcare have contributed time and materials to this project. The University of California, Davis and United Imaging Healthcare have a research agreement and a revenue sharing agreement.

ACKNOWLEDGEMENTS

This EXPLORER scanner was developed with support from NCI, NIBIB and the NIH Office of the Director through Transformative R01 CA 206187, with additional support from United Imaging Healthcare. Support for the human imaging studies presented here was provided by

United Imaging Healthcare and Zhongshan Hospital, Shanghai. We gratefully acknowledge the technical (nursing) assistance of Xiangqing Wang in conducting these studies. We also gratefully acknowledge the EXPLORER team at UC Davis, the entire engineering team at United Imaging Healthcare, our collaborators in the EXPLORER consortium at the University of Pennsylvania and all those, who directly, or indirectly, have helped make this project possible.

REFERENCES

- [1] S. R. Cherry, R. D. Badawi, J. S. Karp, W. W. Moses, P. Price, and T. Jones, "Total-body imaging: Transforming the role of positron emission tomography," *Science Translational Medicine*, vol. 9, article number eaaf6169, March 15, 2017.
- [2] S. R. Cherry, T. Jones, J. S. Karp, J. Qi, W. W. Moses, and R. D. Badawi, "Total-Body PET: Maximizing Sensitivity to Create New Opportunities for Clinical Research and Patient Care," *Journal of Nuclear Medicine*, vol. 59, pp. 3-12, January 1, 2018.
- [3] J. K. Poon, M. L. Dahlbom, W. W. Moses, K. Balakrishnan, W. Wang, S. R. Cherry, *et al.*, "Optimal whole-body PET scanner configurations for different volumes of LSO scintillator: a simulation study," *Physics in Medicine and Biology*, vol. 57, p. 4077-4094, June 7, 2012.
- [4] R. D. Badawi, J. K. Poon, S. Surti, X. Zhang, J. S. Karp, W. W. Moses, *et al.*, "EXPLORER, an Ultrasensitive Total-Body PET Scanner: Application Feasibility Simulations.," presented at the World Molecular Imaging Congress, Savannah, Georgia, 2013.
- [5] V. Viswanath, M. E. Daube-Witherspoon, J. P. Schmall, S. Surti, M. E. Werner, G. Muehllehner, *et al.*, "Development of PET for Total-body Imaging," *Acta Physica Polonica B*, vol. 48, pp. 1555-1566, 2017.
- [6] J. Karp, J. Schmall, M. Geagan, M. Werner, M. Parma, S. Matej, *et al.*, "Imaging Performance of the PennPET Explorer scanner," *Journal of Nuclear Medicine*, vol. 59S, p. 222, May 1, 2018.
- [7] R. Badawi, W. Liu, E. Berg, Y. Lv, T. Xu, S. An, *et al.*, "Progress on the EXPLORER project: towards a total body PET scanner for human imaging," *Journal of Nuclear Medicine*, vol. 59S, p. 223, May 1, 2018.

- [8] Y. Lv, X. Lv, W. Liu, M. S. Judenhofer, A. Zwingenberger, E. R. Wisner, *et al.*, "Mini EXPLORER II: a prototype high-sensitivity PET/CT scanner for companion animal whole body and human brain scanning," *Physics in Medicine & Biology*; *epub ahead of print*, <https://doi.org/10.1088/1361-6560/aafc6c>, 2019.
- [9] "NEMA Standards Publication NU 2-2018, Performance Measurements of Positron Emission Tomographs (PETs)," ed. Roslyn, VA: National Equipment Manufacturer's Association, 2018.
- [10] G. Brix, U. Lechel, G. Glatting, S. I. Ziegler, W. Münzing, S. P. Müller, *et al.*, "Radiation Exposure of Patients Undergoing Whole-Body Dual-Modality ¹⁸F-FDG PET/CT Examinations," *Journal of Nuclear Medicine*, vol. 46, pp. 608-613, April 1, 2005.



Figure 1: Photograph of the completed EXPLORER Total-Body PET/CT scanner.

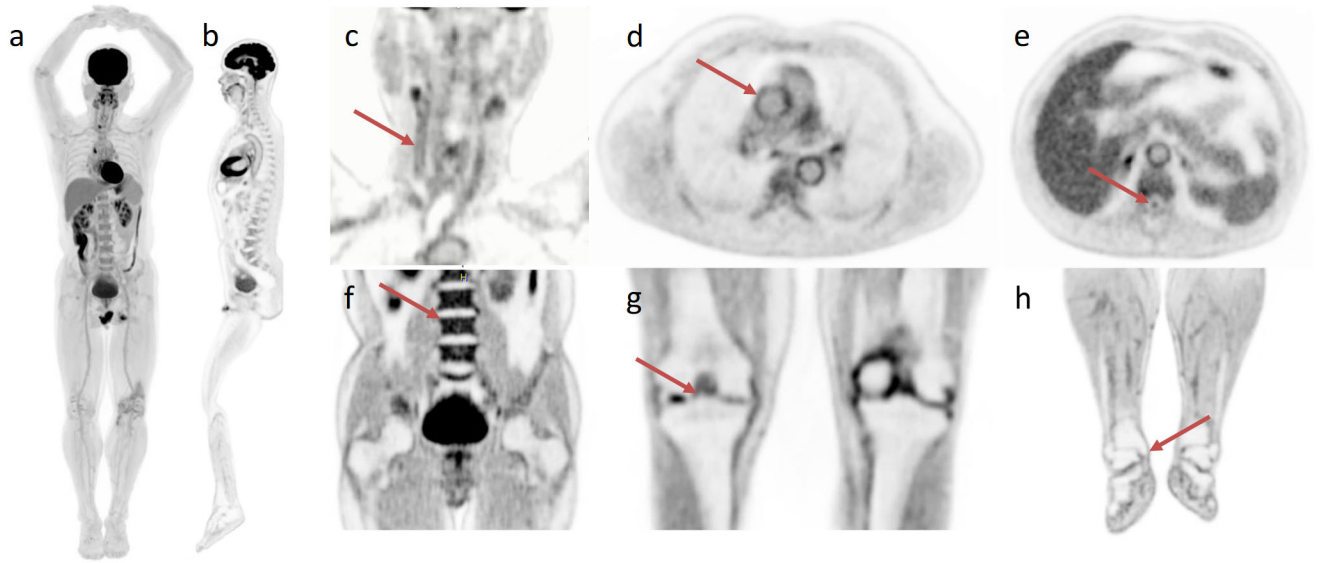


Figure 2. Selected views from the total-body scan of subject 1: (a) total-body MIP; (b) total-body sagittal view; (c) head/neck view, with arrow indicating the walls of the right carotid artery; (d) chest view, showing walls of the major blood vessels, with the ascending aorta indicated by arrow; (e) mid-thoracic view with spinal canal indicated by arrow; (f) abdomen and pelvis, showing clear delineation of the endplates of the vertebral bodies (arrow points to superior endplate of L3); (g) knees with a bone spur indicated by arrow ; (h) lower extremities, with arrow showing delineation of the medial tibial malleolus.

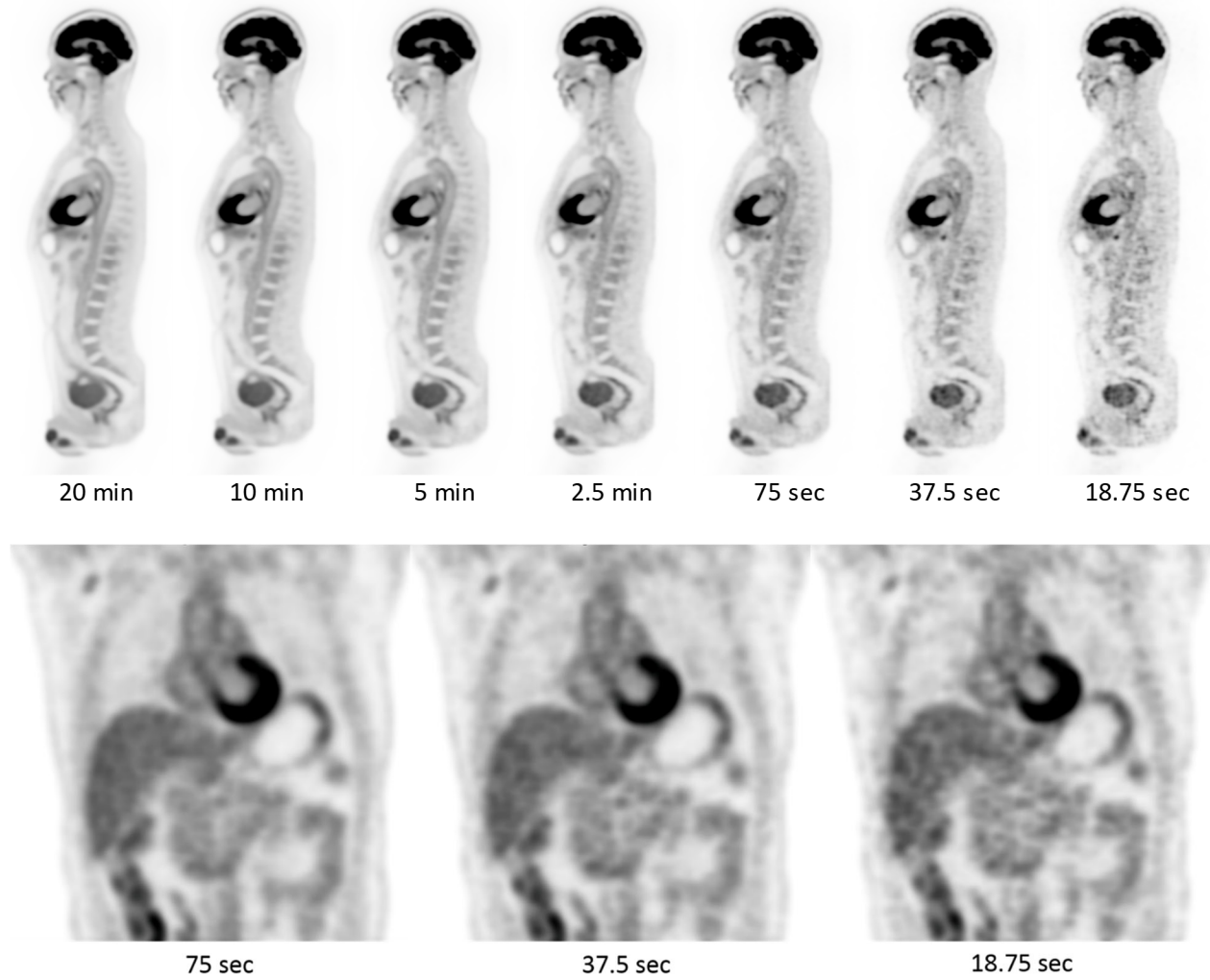


Figure 3. Views from subject 1 as a function of scan duration. 290 MBq injected, 82 mins uptake period. Top: Sagittal views from 20 mins to 18.75 sec. Bottom: Coronal views at 75 sec, 37.5 sec and 18.75 sec.

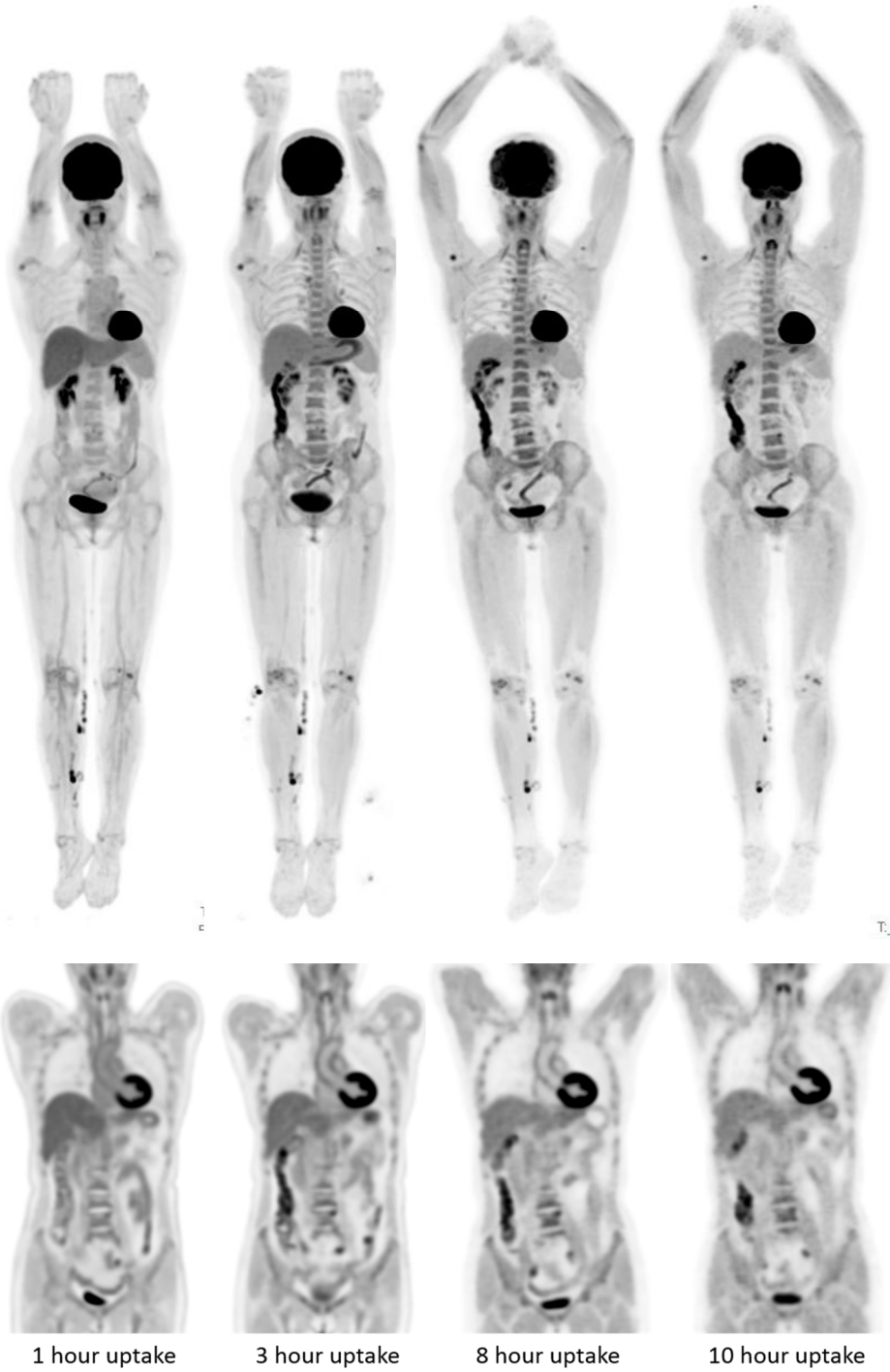


Figure 4. Delayed imaging. 256 MBq injected, 14 minute scan duration. Left-to-right: images from scans performed at 1, 3, 8 and 10 hours post-injection. Top row: MIP images. Bottom row: coronal views of thorax and abdomen. Head motion artifacts are visible in the 8-hour scan.

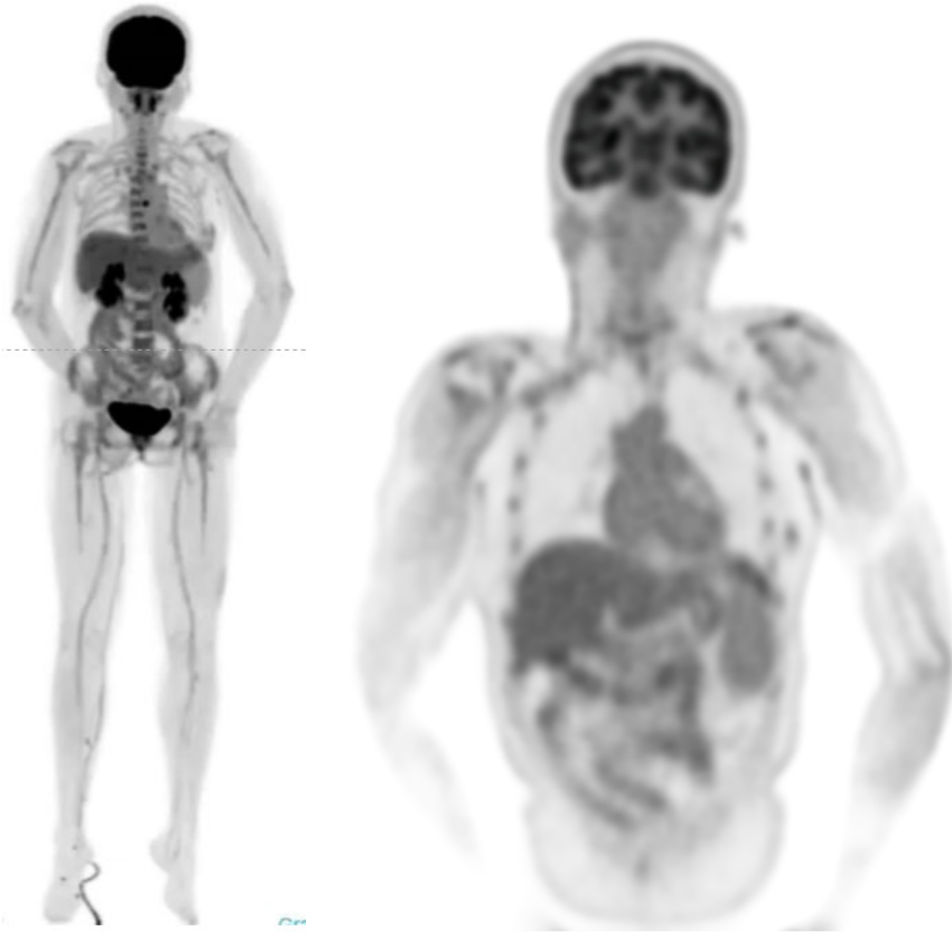


Figure 5. Low-dose images. Subject was injected with 25 MBq and scanned for 10 mins after 52.5 mins of uptake time. Total-body MIP (left) and coronal view of upper body (right). Tracer was injected into a vein in the right lower leg.

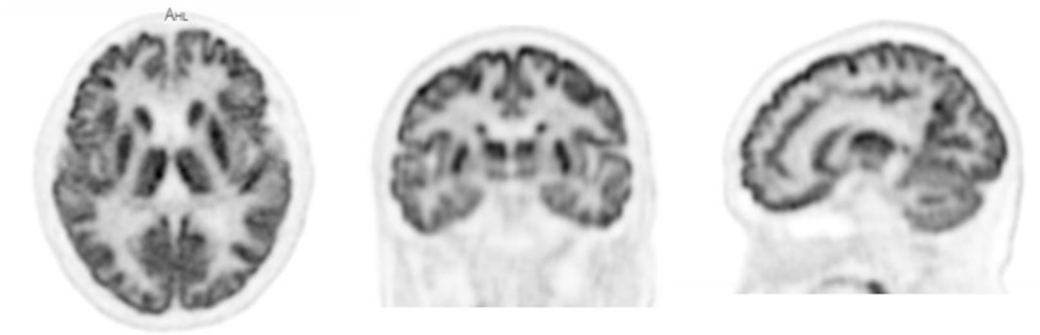


Figure 6. Dedicated brain scan from subject 3. Motion correction has not been implemented at this time.

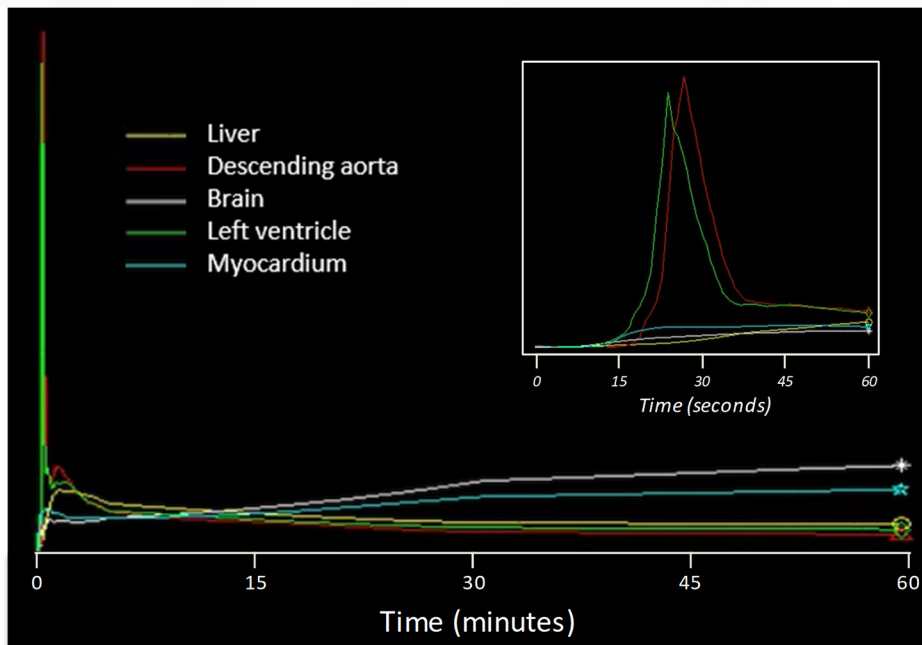
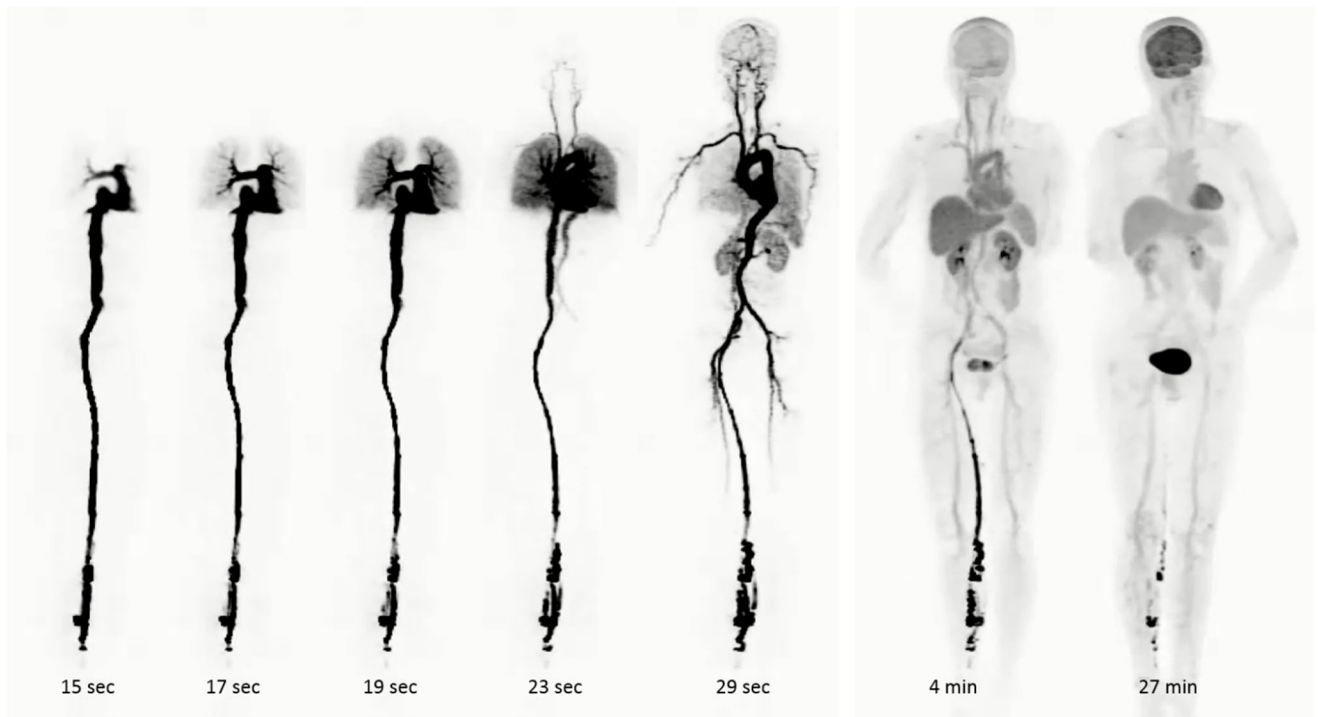


Figure 7. Total-body dynamic imaging. Top: selections of rotating MIPs from the dynamic scan of subject 2. Frame duration is 1 second, except for the 2 left-most images, which have frame durations of 1 minute. Bottom: Time-activity curves (TACs) for selected anatomical regions. Bottom inset: TACs for the first minute of the acquisition.

Subject number	Sex	Age (years)	Weight (kg)	Height (cm)	Blood glucose level (mmol/l)	Injected activity (MBq) (<i>mCi</i>)
1	Male	61	65	163.5	4.9	290 (7.8)
2	Female	61	56	156.0	4.8	256 (6.9)
3	Female	63	55	150.0	4.3	81 (2.2)
4	Female	45	43.5	152.0	5.1	25 (0.68)

Table 1. Subject demographics and injected activity.